Impact of SiO_2 surface composition on trimethylsilane passivation for area-selective deposition

Job Soethoudt[1,2], Steven Crahaij[1,2], Thierry Conard[2], Annelies Delabie[1,2*]

[1] Department of Chemistry, KU Leuven (University of Leuven), 3001, Leuven, Belgium
[2] Imec, Kapeldreef 75, 3001, Leuven, Belgium
** Annelies.Delabie@imec.be*

Abstract

Alkyl-terminated surfaces have received significant interest as growth-blocking surfaces in area-selective deposition (ASD). Gas-phase chemical functionalization is attractive in this context due to its short process times, potentially wide applicability, and ease of integration in industrial process flows. However, the relation between the surface chemistry, the passivating agent, and the growth-blocking efficacy of such treatments is not well understood which can lead to suboptimal passivation performance. This work investigates the reaction between dimethylamino-trimethylsilane (DMA-TMS) and SiO_2 surfaces with varying composition, and identifies the impact of surface composition on passivation efficacy and selectivity. DMA-TMS reacts rapidly with Si-OH groups on SiO_2 in a self-limiting surface reaction, resulting in an -O-Si(CH_3)$_3$ covered surface. In contrast, Si-O-Si groups are either unreactive or significantly less reactive towards DMA-TMS. Increasing the number of Si-OH versus Si-O-Si groups on the initial SiO_2 surface therefore results in a higher -O-Si(CH_3)$_3$ density after DMA-TMS treatment. As a consequence, the selectivity of an ASD process towards SiO_2 improves, as demonstrated for ruthenium atomic layer deposition from 1-ethylbenzyl-1,4-cyclohexadienyl-ruthenium and oxygen. This work illustrates the impact of tuning surface composition on passivation and selectivity for ASD.

Introduction

Area-Selective Deposition (ASD) is a bottom-up patterning approach in which material is selectively deposited on one surface with respect to another surface. ASD is of interest for a variety of applications including self-aligned deposition[1–3], bottom-up filling of 3D structures[4–7], and catalysis[8–11]. In order to enable ASD, the surface dependence of a chemical deposition process needs to be exploited. This is often achieved by rendering one or more surfaces unreactive towards the deposition process, for instance by rendering the surface alkyl-terminated[1,7,12–20]. Alkyl-terminated surfaces can inhibit a wide variety of deposition processes based on metalorganic and halide precursors with a variety of coreagents[7,13–16]. As a consequence, alkyl-terminated surfaces are often selected as the non-growth surface of choice for ASD[1,7,12,14–16].

Surface alkyl groups can be present on as-deposited substrate materials and provide inherent selectivity, for example on organosilicate glass and amorphous carbon films[4,7,13]. In other cases, passivating groups need to be added to achieve selectivity. This can be achieved by organic molecules designed to form a Self-Assembled Monolayer (SAM)[1,16], or adsorption of small alkylating agents such as acetylacetone and a variety of alkylsilanes[2,6,12,14,15]. The molecules in a SAM consist of a head group which reacts with the surface, and tails which organise themselves in a tightly packed layer due to van der Waals forces. This dense layer physically blocks access to the underlying surface, and can therefore be used as passivation layer in ASD when the deposition precursors do not react with the SAM tail groups. Moreover, the large size of the blocking layer can be advantageous for instance when passivating areas on a flat substrate, as the SAM not only prevents deposition on the non-growth surface but also prevents lateral overgrowth of material deposited selectively on the growth surface.

The large size of the SAM can also be a disadvantage in sub-10 nm and 3D structures, as any space occupied by the SAM may not be occupied by the selectively deposited material. Short alkylating agents on the other hand passivate a non-growth surface by directly grafting groups onto the surface with which the deposition precursors do not react. These alkylating agents lack the size and degrees of freedom to display self-assembly, and instead rely on the density and reactivity of sites on the non-growth surface to achieve a maximum packing of nonreactive groups. These small alkylating agents now receive increasing interest because they allow short process times, thermal stability, and compatibility with industrial process flows[17,21,22]. These small passivating agents can also be used to expand the material space for ASD, and to enable advanced ASD processes where the surface passivation is repeatedly applied to improve selectivity[2]. Furthermore, the use of small alkyl groups rather than long chains allows these treatments to be used in sub-10 nm processing, where ASD is expected to become increasingly relevant[23].

A wide range of alkylsilyl compounds react with surface -OH groups to form -O-Si$(CH_3)_x$ groups on SiO_2 surfaces[24–27]. These compounds may therefore be used to enable ASD by selectively passivating SiO_2 surfaces[12,14,15]. Several reports have compared a variety of silylating treatments by their ability to populate the surface with hydrophobic groups[24,27–29], and the -O-Si$(CH_3)_x$ surface group density after silylation has been quantified through Nuclear Magnetic Resonance (NMR)[30,31]. Among dielectric silylating agents, dimethylamino-trimethylsilane (DMA-TMS) is reported to be among the most effective candidates in terms of both final -CH_3 group density and reaction kinetics[27,29]. The latter was attributed to DMA, which is a stronger leaving group compared to its alkoxy- and halide counterparts. Moreover, DMA-TMS displays only a single reactive DMA group. This may be advantageous as during DMA-TMS reaction with SiO_2, this reactive group is consumed yielding DMAH, while the -Si$(CH_3)_3$ group grafted onto the surface displays no additional reactive groups. In contrast, multifunctional agents need to react with multiple surface groups in close vicinity, which may not always be available especially in the high coverage regime of the self-limiting surface reaction[12,26]. The residual reactive groups on these agents may act as reactive sites during subsequent ASD and cause selectivity loss. In this work we therefore focus on monofunctional agents such as DMA-TMS. DMA-TMS reacts with Si-OH groups on SiO_2 via the following reaction[24–27]:

$$SiOH + (CH_3)_2NSi(CH_3)_{3_{(g)}} \rightarrow SiOSi(CH_3)_3 + (CH_3)_2NH_{(g)}$$

However, several aspects of both the SiO_2 silylation reaction and the passivating properties of the resulting surface remain unclear. First, DMA-TMS reactivity towards Si-OH groups is well established, yet the reactivity of DMA-TMS towards surface Si-O-Si groups has not yet been reported. SiO_2 surfaces are typically composed of both Si-OH and Si-O-Si groups, and their relative concentration depends on the preparation method and temperature[32,33]. An exchange reaction between DMA-TMS and Si-O-Si is possible, as the bonds broken in this exchange reaction are the same as the ones which are formed, specifically one Si-O and one Si-N bond. Whether or not this reaction occurs could significantly affect the final Si-CH_3 group density. Second, while silylating agents receive increasing interest for SiO_2 passivation in ASD, various SiO_2 preparation methods are used while the impact of SiO_2 surface composition on selectivity has to the best of our knowledge not been discussed.

This work aims to expand the current understanding of the surface reactions between DMA-TMS and SiO_2, and its impact on selectivity. The objectives of this work are twofold. First, we investigate the reactivity of DMA-TMS towards Si-O-Si bridges to obtain a more complete understanding of the reaction of DMA-TMS with SiO_2 surfaces. Changes in the SiO_2 surface composition during silylation are quantified using independent methods to measure surface -OH and -O-Si$(CH_3)_3$ group density respectively, and the achieved density of passivating -O-Si$(CH_3)_3$ groups is compared to the calculated limit of steric hindrance. Second, we assess the impact of surface preparation on selectivity for ASD. We use 1-ethylbenzyl-1,4-cyclohexadienylruthenium and oxygen (EBECHRu/O_2) Atomic Layer Deposition (ALD) because it displays different reactivity towards Si-OH, Si-O-Si, and Si-CH_3 groups, with Si-CH_3 groups being far less reactive compared to Si-OH and Si-O-Si groups[13]. This allows us to directly quantify the impact of surface preparation on growth inhibition caused by DMA-TMS and its impact on selectivity.

Results and Discussion

Functionalisation of SiO_2 surfaces by DMA-TMS

First the theoretical steric maximum density of passivating -O-Si(CH_3)$_3$ groups on a 2D surface is determined, to provide a reference for the experimental observations that follow. To calculate this steric limit we assume closed packing of -CH_3 groups at the surface. In reality, the random adsorption of silylating agents can lead to suboptimal space occupation, and the final -CH_3 coverage is expected to be below the close packed value[12]. Nevertheless, a comparison to the steric limit of passivating -CH_3 group density is useful when interpreting differences in passivation efficacy for ASD. Organizing surface groups in a 2D hexagonally close packed (hcp) order yields a maximum areal coverage fraction $\theta_{max} = 0.9069$[34]. Dividing θ_{max} by the projected 2D area of a single -CH_3 group A_{CH3} yields the maximum surface density of -CH_3 groups $\Gamma_{CH_3,max}$. The area A_{CH3} in turn is calculated from the van der Waals radius of a -CH_3 group $r_{vdw} = 0.200\ nm$[35]. For the reaction between DMA-TMS and surface -OH groups, the functional group is -O-Si(CH_3)$_3$ which contains three -CH_3 groups. Dividing $\Gamma_{CH_3,max}$ by three yields the theoretical maximum density of -O-Si(CH_3)$_3$ groups $\Gamma_{-OSi(CH_3)_3,max}$. A steric limit of 2.41 -O-Si(CH_3)$_3$ nm^{-2} is obtained, which is comparable to the 2.2-2.8 nm^{-2} reported by Sindorf and Maciel[31].

$$\Gamma_{-O-Si(CH_3)_3,max} = \frac{\Gamma_{CH_3,max}}{3} = \frac{1}{3}\frac{\theta_{max}}{A_{CH3}} = \frac{1}{3}\frac{\theta_{max}}{\pi {r_{vdw}}^2} = 2.41\ -OSi(CH_3)_3\ nm^{-2}$$

We first evaluate the evolution of the surface reaction on an -OH-rich Plasma-Enhanced ALD (PEALD) SiO_2 surface, as DMA-TMS readily reacts with -OH groups[13]. The -OH group density on a SiO_2 surface is quantified by letting each -OH group react with $HfCl_4$ in an ALD reactor, followed by Hf areal density quantification by Rutherford Backscattering Spectrometry (RBS)[36]. The PEALD SiO_2 surface displays 2.5 -OH/nm^2, exceeding the steric limit of -O-Si(CH_3)$_3$ groups which can be accommodated at the surface. It is therefore a good starting surface for evaluating the surface reaction between DMA-TMS and Si-OH groups. The DMA-TMS treatment temperature of 250 ˚C is not expected to affect the surface -OH group density significantly, as 250 ˚C is too low for significant dehydroxylation to occur[37]. Water Contact Angle (WCA) measurements show that the DMA-TMS surface reaction saturates within 300 s on this surface (Figure 1a). To quantify the evolution of surface groups, the -OH and -O-Si(CH_3)$_3$ group density are independently measured after varying DMA-TMS exposure times between 0 s and 500 s (Figure 1b). The -OH group density was obtained from $HfCl_4$ exposure and subsequent Hf RBS, while the -O-Si(CH_3)$_3$ group density was obtained from the Si2p peak in X-Ray Photoelectron Spectroscopy (XPS) by comparing the SiO_2 peak and -O-Si(CH_3)$_3$ shoulder intensities through a surface contamination model[38] (Figure 2). Surface -OH groups are gradually replaced by -O-Si(CH_3)$_3$ groups, and XPS shows that the surface reaction saturates when about 2 -O-Si(CH_3)$_3$ groups/nm^2 are formed, close to the steric limit. As each -O-Si(CH_3)$_3$ group corresponds to three -CH_3 groups, the DMA-TMS treated SiO_2 surface is covered with 6 -CH_3/nm^2. Note that while the sum of surface -OH groups and -O-Si(CH_3)$_3$ groups remains constant, roughly 0.4 -OH/nm^2 remain at the surface and do not react with DMA-TMS. We attribute this remaining unreacted -OH group density to the steric limitation calculated earlier. In short, the surface reaction between DMA-TMS and surface -OH groups is self-limiting, and -OH groups are only replaced as long as new -O-Si(CH_3)$_3$ groups can still be accommodated at the surface.

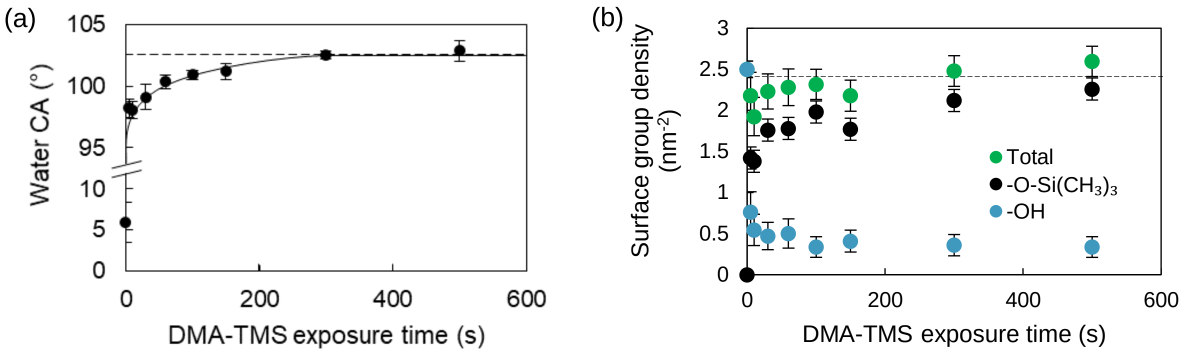

Figure 1: DMA-TMS populates an -OH-rich SiO_2 surface with -O-Si(CH_3)$_3$ in ~300 s. a) surface saturation of the DMA-TMS treatment on SiO_2 as determined by WCA, b) change in SiO_2 surface groups for increasing DMA-TMS exposure time. -OH density was measured by exposing the DMA-TMS treated surface to $HfCl_4$ followed by Hf RBS, while -O-Si(CH_3)$_3$ density after DMA-TMS reaction was quantified by X-ray Photoelectron Spectroscopy (XPS). A solid line is provided as guide to the eye.

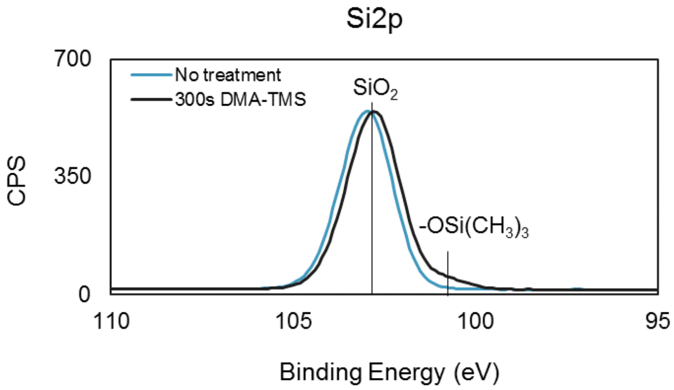

Figure 2: Overlay of SiO_2 Si2p XPS spectra with and without 300 s DMA-TMS treatment. The spectrum after DMA-TMS treatment displays a shoulder corresponding to a submonolayer of -O-Si(CH_3)$_3$ groups, which can be used to calculate the number density of these groups through a surface contamination model[38].

Next, the reactivity of DMA-TMS towards Si-O-Si groups is compared to that of Si-OH groups. Cleaned thermal SiO_2 surfaces are annealed at different temperatures ranging from 300 °C to 850 °C to create surfaces with different surface composition (Figure 3a). The as-cleaned surface (no anneal) is represented as 25 °C, and the as-grown thermal oxide is represented at the growth temperature of 1000 °C. Increasing the annealing temperature decreases the Si-OH group density and increases Si-O-Si group density, as silanols condense into siloxane bridges through the mechanism 2Si-OH → Si-O-Si + H_2O[32]. The SiO_2 surface composition affects the number of -O-Si(CH_3)$_3$ groups placed during DMA-TMS treatment (Figure 3b). For SiO_2 surfaces with high -OH group densities, -O-Si(CH_3)$_3$ group densities close to the steric limit are obtained. On the other hand, for SiO_2 surfaces with low -OH group densities, the -O-Si(CH_3)$_3$ group density decreases with this initial –OH group density. This signals the critical role of surface -OH groups in facilitating surface silylation. From these observations we conclude that Si-O-Si groups are unreactive or at least significantly less reactive compared to -OH groups in the same timescales. For low -OH group densities, the slope of the -O-Si(CH_3)$_3$ vs -OH curve is below unity, which means that only some of the -OH groups react with DMA-TMS. As a result, 2.5 -OH/nm^2 are required to yield 2 -O-Si(CH_3)$_3$/nm^2. This may be partly attributed to steric hindrance on geminal Si-OH groups, which form a minority fraction of the surface -OH groups at these anneal temperatures[37]. Hydrogen bonding between Si-OH groups is not expected to limit their reactivity towards DMA-TMS, as aminosilanes are more reactive than both chlorosilanes and alkoxysilanes[27,29], and chlorosilanes react readily with both hydrogen-bonded and non-hydrogen-bonded silanols, while a difference in reactivity was observed only for the less reactive methoxysilanes[39]. Moreover, the samples with less than 2 OH/nm^2 are annealed at >500 °C, above which the number of hydrogen bonded silanols is negligible[37]. These findings suggest that when a high -O-Si(CH$_3$)$_3$ group density is desired, for instance when passivating a SiO$_2$ surface for ASD, it is important that the surface preparation results in the highest possible -O-Si(CH$_3$)$_3$ group coverage, as is observed for -OH group densities higher than 2.5 -OH/nm^2.

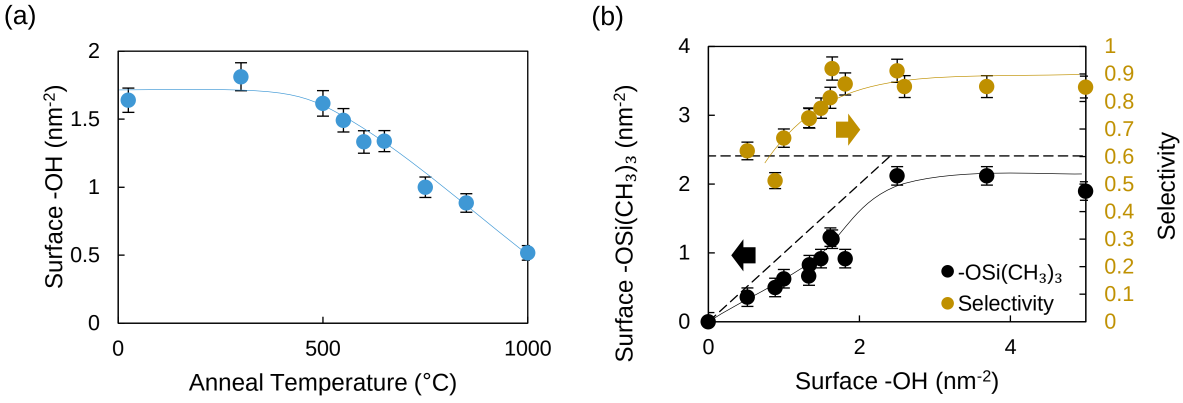

Figure 3: The ability of DMA-TMS to block growth on SiO$_2$ depends strongly on the initial surface -OH group density on the dielectric surface. a) evolution of SiO$_2$ surface -OH group density with annealing temperature as determined by HfCl$_4$ exposure and subsequent Hf RBS. b) impact of the SiO$_2$ -OH group density on both -O-Si(CH$_3$)$_3$ group coverage after DMA-TMS treatment, and the selectivity for a 5 nm Ru layer grown on DMA-TMS treated TiN as growth surface selectively to a DMA-TMS treated SiO$_2$ non-growth surface. The selectivity is determined as the normalized difference between the amount of material on the growth and non-growth surface[40]. Data on a TiN growth surface was acquired by applying a 300 s DMA-TMS treatment followed by 100 Ru ALD cycles. Solid lines are provided as a guide to the eye. The dashed line corresponds to the theoretical maximum surface density of -O-Si(CH$_3$)$_3$ groups, which is limited by the amount of available -OH groups at < 2.41 -OH/nm^2 and by steric hindrance at densities > 2.41 -OH/nm^2.

Influence of -O-Si(CH$_3$)$_3$ group density on surface passivation for Ru ALD

Lastly, we investigate the influence of the -O-Si(CH$_3$)$_3$ group density on the selectivity of Ru ALD. EBECHRu/O$_2$ ALD displays inhibited growth on dielectrics, and the amount of material deposited during the initial regime is extremely sensitive to the dielectric surface termination[13]. EBECHRu/O$_2$ is therefore well-suited to demonstrate the impact of SiO$_2$ surface group variations on growth inhibition. Selectivity can only be obtained by comparing the SiO$_2$ non-growth surface to a growth surface. TiN was therefore used as a reference growth surface for all selectivity experiments, as EBECHRu/O$_2$ proceeds linearly on this surface without any inhibition[41].

Because chemical selectivity is challenging to measure and difficult to quantitatively relate to the observed surface-dependent growth behaviour, various groups have recently adopted a metric for selectivity which is easy to measure, allows results from different processes and characterization methods to be compared, and provides relevant information for ASD. By comparing the normalised difference between the amount of material on a growth and non-growth surface, surface-dependent growth behaviour can be quantified for a given thickness of the selectively grown layer. Selectivity is typically close to unity during the initial stages of deposition and degrades with increasing ASD layer thickness as more unwanted deposition occurs on the non-growth surface[40]. In this study, a high enough ASD thickness (5 nm) is chosen for selectivity to deviate significantly from unity, so that differences in selectivity due to changes in initial SiO_2 surface composition are more easily compared. While the growth behaviour on homogeneous substrates may differ from the growth behaviour on a patterned, heterogeneous substrate, the surface-dependent growth behaviour observed on homogeneous substrates provides valuable information about the impact of surface chemistry on growth for both non-patterned and patterned substrates alike. In this work for instance, growth data from homogeneous substrates are used to understand the impact of SiO_2 surface composition on selectivity. This understanding is of critical importance for application on industrially relevant patterned substrates, as nanopattern fabrication involves frequent wet, plasma, and thermal treatments all of which can affect the SiO_2 surface composition.

The -O-Si(CH_3)$_3$ group density strongly influences the selectivity of Ru ALD (Figure 3b). When the initial SiO_2 surface -OH group density is low (<< 2 -OH/nm^2), few passivating -O-Si(CH_3)$_3$ groups will be placed on the surface which results in low selectivity. This can be attributed to Ru deposition on exposed Si-O-Si bridges between -O-Si(CH_3)$_3$ groups, as Ru deposits much more rapidly on Si-O-Si bridges compared to Si-CH_3[13]. Another possible reason for selectivity loss stems from the combustion reactions during the EBECHRu/O_2 ALD process itself. These combustion reactions generate H_2O, which can hydroxylate exposed Si-O-Si bridges to Si-OH groups[41]. While Si-OH groups are desirable during the DMA-TMS passivation step, Si-OH groups generated from Si-O-Si bridges during Ru ALD itself result in selectivity loss because EBECHRu/O_2 ALD proceeds more rapidly on Si-OH compared to Si-O-Si terminated surfaces[13]. A fully -O-Si(CH_3)$_3$ terminated surface does not suffer from this disadvantage, as surface -CH_3 groups are not affected by H_2O exposure at 325 ˚C[13]. While selectivity is low when few initial -OH groups are present during DMA-TMS passivation, selectivity improves with increasing initial -OH group density, and the selectivity is highest when the -O-Si(CH_3)$_3$ group density approaches the limit of steric hindrance. These results illustrate the pivotal role of SiO_2 surface composition on the extent of silylation by DMA-TMS, and its impact on selectivity during EBECHRu/O_2 ALD.

Using an -OH-rich SiO_2 surface rather than a Si-O-Si-rich SiO_2 surface strongly improves selectivity towards SiO_2 as illustrated by Figure 4. The selectivity of EBECHRu/O_2 ALD is shown using TiN as growth surface and various dielectrics as non-growth surface. Treating SiO_2 with DMA-TMS yields a rather limited selectivity increase on Si-O-Si terminated SiO_2, while a much more pronounced increase is observed on Si-OH terminated SiO_2. Surface silylation studies often do not report the initial SiO_2 surface composition, and the findings presented here may serve to partly explain some of the differences in silylation efficacy observed in literature. While DMA-TMS passivation of -OH terminated SiO_2 yields high selectivities for thicknesses up to 5 nm, even higher selectivities are obtained by employing the -CH_3 surface termination inherently present on as-deposited organosilicate glass (OSG)[13]. While the latter may be difficult to employ for ASD on patterned substrates as the patterning process invariably destroys the -CH_3 termination, identifying and reproducing its surface selectively on a nanopattern could improve selectivity beyond what is achievable by alkylsilanes. Additionally, selectivity on nanopatterns may be improved by defect mitigation strategies based on insight in growth mechanisms. These include diffusion of deposited material from the non-growth to the growth surface such as demonstrated in selective epitaxial growth[42], and selective passivation - deposition - defect etch processes, where DMA-TMS has already been used to improve selectivity towards -OH terminated SiO_2[6].

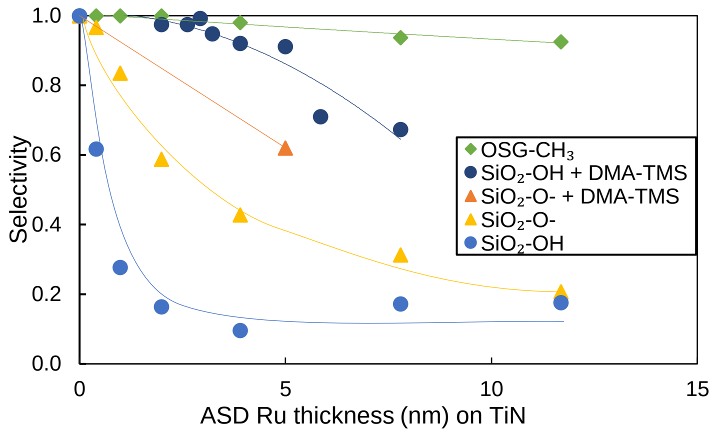

Figure 4: Selectivity for EBECHRu/O_2 ASD on TiN versus various dielectrics as a function of ASD layer thickness on TiN. This surface allows the selectivity induced by DMA-TMS treatment to be compared to selectivity towards various unmodified dielectric surfaces. SiO_2-OH corresponds a PEALD SiO_2 surface with 2.5 -OH/nm^2, while SiO_2-O- corresponds to a dry thermal SiO_2 growth at 1000 ˚C which is primarily Si-O-Si terminated. DMA-TMS corresponds to a 300 s treatment which is sufficient for saturation as illustrated earlier in this work. Solid lines are provided as guide to the eye.

Conclusion

This work demonstrates the relation between SiO_2 surface composition and the passivation efficacy of DMA-TMS for area-selective deposition. During the surface reaction between DMA-TMS and SiO_2, independent quantitative measurements were obtained for the decrease in -OH group density and the increase in density of passivating -O-Si$(CH_3)_3$ groups. On surfaces with OH density > 2.5 -OH/nm^2, the DMA-TMS surface reaction saturates at 2 -O-Si$(CH_3)_3$ nm^{-2}, which is in agreement with the theoretically calculated maximum due to steric hindrance. On the other hand no reaction is observed between DMA-TMS and Si-O-Si groups, and the -O-Si$(CH_3)_3$ group density after DMA-TMS treatment increases with the number of Si-OH groups initially present. As a result, the selectivity of Ru ALD is found to depend strongly on the initial SiO_2 surface composition. For surface -OH group densities below the steric limit of 2 -O-Si$(CH_3)_3$ nm^{-2}, passivation efficacy towards Ru ALD rapidly decreases as the surface is not fully covered by unreactive -CH_3 groups. At least 2.5 -OH/nm^2 are therefore required to passivate a SiO_2 surface with trimethylsilyl groups. We illustrated how tailoring the initial surface preparation to the passivating molecule can help significantly improve passivation and therefore improve selectivity for ASD. Such understanding could significantly aid in the design of industrially relevant processes for ASD, as pattern fabrication steps typically include a range of process steps which affect surface composition, such as thermal treatments and cleaning steps. We also illustrate that current DMA-TMS treatment does not replicate the selectivity towards an inherently dense -CH_3 terminated OSG surface, and further studies on the impact of dielectric surface structure may yield additional selectivity improvements. While this work uses Ru ALD to show illustrate the impact on ASD, this approach could be extended to other materials as -CH_3 groups inhibit a wide variety of deposition processes.

Experimental Details

Dielectric substrates were prepared on 300mm Si (100) wafers. On each Si wafer 100 nm dry thermal SiO_2 was grown at 1000 °C. For the initial study of DMA-TMS exposure on -OH-rich SiO_2, the 100 nm thermal SiO_2 layer was covered with 15 nm hydrophilic SiO_2. The hydrophilic SiO_2 was deposited by PEALD in an ASM Eagle 12 reactor at 75 °C to obtain a dielectric surface with 2.5 -OH/nm^2 [13]. Other substrates covered only with the 100 nm dry thermal SiO_2 were used to study the impact of SiO_2 surface composition on passivation and selectivity. These substrates were cleaned and annealed after thermal oxidation with the aim of modifying the surface -OH density[36]. These substrates were first cleaned in a DNS single wafer cleaning tool by standard cleaning solution SC1[43], and subsequently annealed 30 minutes in N_2 ambient in an ASM Levitor tool with annealing temperatures ranging between 300 °C and 850 °C. Some Si wafers were covered with 10 nm TiN by Physical Vapor Deposition (PVD), achieved by Ti sputtering in N_2 ambient. TiN was used as a reference growth surface to determine selectivity towards DMA-TMS treated SiO_2 as rapid linear growth is observed for EBECHRu/O_2 ALD on TiN[41]. An OSG surface is prepared to compare the effect of surface alkylation by DMA-TMS to selectivity towards an inherently -CH_3 terminated dielectric surface[13]. OSG films are obtained by Plasma-Enhanced Chemical Vapor Deposition (PECVD) of 100 nm OSG film with a density of 1.35 g/cm3 and k-value of 2.8.

Substrates were pretreated with DMA-TMS to investigate the surface reactions and their impact on subsequent ALD. This pretreatment was carried out in static mode in a TEL Tactras system using a showerhead-type reactor. Substrates were kept in 5 Torr N_2 ambient at 250 °C for 10 minutes to desorb moisture and organic species, after which the reactor chamber was evacuated. The chamber was then filled with a mixed flow of 500 sccm DMA-TMS and 350 sccm N_2 to a total pressure of 5 Torr, in which the substrate was kept for varying amounts of time to allow surface reactions to proceed.

ALD was carried out on DMA-TMS treated substrates to study the impact of DMA-TMS treatment on selectivity. A DMA-TMS exposure time of 300 s was selected as this corresponds to the condition for surface saturation established in this work. In each case, substrates were transferred to the ALD reactor immediately after substrate preparation to minimize the effect of air exposure. Furthermore, substrates were kept in the reactor at 325 °C for 5 minutes before ALD to desorb moisture and other contaminants from the surface. Ru was deposited by applying 100 cycles of EBECHRu/O_2 ALD at 325 °C in an ASM Pulsar 3000 chamber connected to a Polygon platform. The pulse sequence used was 5 s EBECHRu pulse, 5 s N_2 purge, 0.4 s O_2 pulse, and 3 s N_2 purge[41].

The reaction between DMA-TMS and each substrate was identified through surface characterization, and the impact on Ru ALD growth inhibition was measured. WCA measurements were performed in a Dataphysics OCAH 230 tool. Surface -OH group density on dielectrics was determined by exposing the substrate to a single $HfCl_4$ pulse, followed by Hf areal density quantification through RBS using a 1.523 MeV He^+ incoming ion beam. As each surface -OH group reacts with only one $HfCl_4$ precursor molecule, the RBS Hf areal density is a measure for the surface -OH density originally present for a range of 0.4 – 2.9 -OH/nm^2 [36]. This method assumes that $HfCl_4$ does not react significantly with -O-Si(CH_3)$_3$ groups within the span of a single pulse. While the validity of this assumption is supported by the absence of a change in -O-Si(CH_3)$_3$ group density after a single $HfCl_4$ pulse as determined by XPS, experiments with ten $HfCl_4$ pulses resulted in observable -O-Si(CH_3)$_3$ group loss of ~10%. We therefore conclude that while the single $HfCl_4$ pulses primarily probe surface -OH group density, a small undesired contribution from interaction with -O-Si(CH_3)$_3$ groups cannot be excluded. This method used to measure -OH group density is valid up to 2.9 -OH/nm^2, as higher -OH group densities result in steric hindrance between $HfCl_x$ surface species, or $HfCl_4$ molecules reacting with multiple adjacent -OH groups due to their proximity.

Surface -O-Si(CH_3)$_3$ group quantification is carried out through Si XPS, in which the surface group density is obtained from the Si2p spectrum through a surface contamination model[38]. Example XPS spectra of SiO_2 before and after DMA-TMS treatment are shown in Figure 2, illustrating the presence of a SiO shoulder in the Si2p peak after treatment. This shoulder represents a submonolayer of -O-Si(CH_3)$_3$ surface groups and is used in the surface contamination model. XPS was performed with a Thermo Scientific Theta 300 spectrometer using a 1486.6 eV monochromatized Al Kα X-ray source. The change in surface -O-Si(CH_3)$_3$ group content was measured by XPS using the same procedure as during surface characterization. Accurate comparison of -O-Si(CH_3)$_3$ group densities between XPS spectra is facilitated by using a constant peak fitting procedure which fixes the SiO_2 and -O-Si(CH_3)$_3$ peak shapes as well as their relative position for all spectra. Moreover all data were collected in a single measurement series to minimize variability due to long-term sensitivity fluctuations, so that the uncertainty consists mainly of statistical and reproducibility errors which were quantified by repeated measurements on a SiO_2 sample treated with DMA-TMS for 300 s.

The amount of Ru deposited on DMA-TMS treated SiO_2 surfaces was quantified by RBS using an incoming 1.523 MeV He^+ ion beam. The selectivity predictions are calculated by normalizing the difference in amount of Ru deposited on a DMA-TMS treated TiN growth surface and DMA-TMS treated SiO_2 non-growth surface as measured by RBS. This method allows to compare the surface dependence of different deposition processes and on different surfaces, and is therefore a valuable tool for the identification and improvement of ASD processes[40,44]. TiN is chosen as growth surface because EBECHRu/O_2 ALD displays linear enhanced growth on TiN[41], but only serves as a reference point to study the impact of SiO_2 surface composition on selectivity. All selectivity values shown correspond to a 5 nm Ru film on DMA-TMS treated TiN, deposited by 100 cycles of Ru ALD.

References

(1) Mackus, A. J. M.; Bol, A. A.; Kessels, W. M. M. The Use of Atomic Layer Deposition in Advanced Nanopatterning. *Nanoscale* **2014**, *6* (19), 10941–10960.

(2) Mameli, A.; Merkx, M. J. M.; Karasulu, B.; Roozeboom, F.; Kessels, W. M. M.; Mackus, A. J. M. Area-Selective Atomic Layer Deposition of SiO2 Using Acetylacetone as a Chemoselective Inhibitor in an ABC-Type Cycle. *ACS Nano* **2017**, *11* (9), 9303–9311.

(3) Biyikli, N.; Haider, A.; Deminskyi, P.; Yilmaz, M. Self-Aligned Nanoscale Processing Solutions via Selective Atomic Layer Deposition of Oxide, Nitride, and Metallic Films. In *Low-Dimensional Materials and Devices 2017*; Kobayashi, N. P., Talin, A. A., Davydov, A. V., Islam, M. S., Eds.; SPIE, 2017; Vol. 10349, p 20.

(4) Zyulkov, I.; Krishtab, M.; De Gendt, S.; Armini, S. Selective Ru ALD as a Catalyst for Sub-Seven-Nanometer Bottom-Up Metal Interconnects. *ACS Appl. Mater. Interfaces* **2017**, *9* (36), 31031–31041.

(5) Sprenger, J. K.; Sun, H.; Cavanagh, A. S.; Roshko, A.; Blanchard, P. T.; George, S. M. Electron-Enhanced Atomic Layer Deposition of Boron Nitride Thin Films at Room Temperature and 100 °C. **2018**.

(6) Soethoudt, J.; Hody, H.; Spampinato, V.; Franquet, A.; Briggs, B.; Chan, B. T.; Delabie, A. Defect Mitigation in Area-Selective Atomic Layer Deposition of Ruthenium on Titanium Nitride/Dielectric Nanopatterns. *Adv. Mater. Interfaces* **2019**, 1900896.

(7) Stevens, E.; Tomczak, Y.; Chan, B. T.; Altamirano Sanchez, E.; Parsons, G. N.; Delabie, A. Area-Selective Atomic Layer Deposition of TiN, TiO $_2$, and HfO $_2$ on Silicon Nitride with Inhibition on Amorphous Carbon. *Chem. Mater.* **2018**, *30* (10), 3223–3232.

(8) Liu, X.; Zhu, Q.; Lang, Y.; Cao, K.; Chu, S.; Shan, B.; Chen, R. Oxide-Nanotrap-Anchored Platinum Nanoparticles with High Activity and Sintering Resistance by Area-Selective Atomic Layer Deposition. *Angew. Chemie* **2017**, *129* (6), 1670–1674.

(9) Aragao, I. B.; Ro, I.; Liu, Y.; Ball, M.; Huber, G. W.; Zanchet, D.; Dumesic, J. A. Catalysts Synthesized by Selective Deposition of Fe onto Pt for the Water-Gas Shift Reaction. *Appl. Catal. B Environ.* **2018**, *222*, 182–190.

(10) Cheng, N.; Banis, M. N.; Liu, J.; Riese, A.; Li, X.; Li, R.; Ye, S.; Knights, S.; Sun, X. Extremely Stable Platinum Nanoparticles Encapsulated in a Zirconia Nanocage by Area-Selective Atomic Layer Deposition for the Oxygen Reduction Reaction. *Adv. Mater.* **2015**, *27* (2), 277–281.

(11) Cao, K.; Zhu, Q.; Shan, B.; Chen, R. Controlled Synthesis of Pd/Pt Core Shell Nanoparticles Using Area-Selective Atomic Layer Deposition. *Sci. Rep.* **2015**, *5* (1), 8470.

(12) Khan, R.; Shong, B.; Ko, B. G.; Lee, J. K.; Lee, H.-B.-R. B. R. H.; Park, J. Y.; Oh, I.-K. K.; Raya, S. S.; Hong, H. M.; Chung, K.-B. B.; et al. Area-Selective Atomic Layer Deposition Using Si Precursors as Inhibitors. *Chem. Mater.* **2018**, *30* (21), 7603–7610.

(13) Soethoudt, J.; Grillo, F.; Marques, E. A. E. A.; van Ommen, J. R. R.; Tomczak, Y.; Nyns, L.; Van Elshocht, S.; Delabie, A. Diffusion-Mediated Growth and Size-Dependent Nanoparticle Reactivity during Ruthenium Atomic Layer Deposition on Dielectric Substrates. *Adv. Mater. Interfaces* **2018**, 1800870.

(14) Au, Y.; Lin, Y.; Kim, H.; Beh, E.; Liu, Y.; Gordon, R. G. Selective Chemical Vapor Deposition of Manganese Self-Aligned Capping Layer for Cu Interconnections in Microelectronics. *J. Electrochem. Soc.* **2010**, *157* (6), D341.

(15) Elko-Hansen, T. D.-M.; Ekerdt, J. G. (Invited) *Selective Atomic Layer Deposition of Cobalt for Back End of Line*. *ECS Trans.* **2017**, *80* (3), 29–37.

(16) Minaye Hashemi, F. S.; Prasittichai, C.; Bent, S. F. Self-Correcting Process for High Quality Patterning by Atomic Layer Deposition. *ACS Nano* **2015**, *9* (9), 8710–8717.

(17) Chen, R.; Kim, H.; McIntyre, P. C.; Bent, S. F. Investigation of Self-Assembled Monolayer Resists for Hafnium Dioxide Atomic Layer Deposition. *Chem. Mater.* **2005**, *17* (3), 536–544.

(18) Heo, J.; Won, S.-J.; Eom, D.; Lee, S. Y.; Ahn, Y. B.; Hwang, C. S.; Kim, H. J. The Role of the Methyl and Hydroxyl Groups of Low-k Dielectric Films on the Nucleation of Ruthenium by ALD. *Electrochem. Solid-State Lett.* **2008**, *11* (8), H210.

(19) Satta, A.; Baklanov, M.; Richard, O.; Vantomme, A.; Bender, H.; Conard, T.; Maex, K.; Li, W. M.; Elers, K. E.; Haukka, S. Enhancement of ALCVD(TM) TiN Growth on Si-O-C and [Alpha]-SiC:H Films by O2-Based Plasma Treatments. *Microelectron. Eng.* **2002**, *60* (1–2), 59–69.

(20) Matsumoto, K.; Maekawa, K.; Nagai, H.; Koike, J. Deposition Behavior and Substrate Dependency of ALD MnOxdiffusion Barrier Layer. *Proc. 2013 IEEE Int. Interconnect Technol. Conf. IITC 2013* **2013**, 1–3.

(21) Jiang, X.; Bent, S. F. Area-Selective ALD with Soft Lithographic Methods: Using Self-Assembled Monolayers to Direct Film Deposition. *J. Phys. Chem. C* **2009**, *113* (41), 17613–17625.

(22) Junsic, H.; Porter, D. W.; Sreenivasan, R.; McIntyre, P. C.; Bent, S. F. ALD Resist Formed by Vapor-Deposited Self-Assembled Monolayers. *Langmuir* **2007**, *23* (3), 1160–1165.

(23) Mackus, A. J. M. Approaches and Opportunities for Area-Selective Atomic Layer Deposition. In *2018 International Symposium on VLSI Technology, Systems and Application (VLSI-TSA)*; IEEE, 2018; pp 1–2.

(24) Dao, T.; Spence, C. A.; Hess, D. W. Study of Silylation Mechanism and Kinetics through Variations in Silylating Agent and Resin. *Proc. SPIE* **1991**, *1466*, 257–268.

(25) Mor, Y. S.; Chang, T. C.; Liu, P. T.; Tsai, T. M.; Chen, C. W.; Yan, S. T.; Chu, C. J.; Wu, W. F.; Pan, F. M.; Lur, W.; et al. Effective Repair to Ultra-Low-k Dielectric Material (K~2.0) by Hexamethyldisilazane Treatment. *J. Vac. Sci. Technol. B Microelectron. Nanom. Struct.* **2002**, *20* (4), 1334.

(26) Böhm, O.; Leitsmann, R.; Plänitz, P.; Oszinda, T.; Schaller, M.; Schreiber, M. Novel K-Restoring Scheme for Damaged Ultra-Low-k Materials. *Microelectron. Eng.* **2013**, *112*, 63–66.

(27) Imada, T.; Nakata, Y.; Ozaki, S.; Kobayashi, Y.; Nakamura, T. Systematic Investigation of Silylation Materials for Recovery Use of Low- k Material Plasma Damage Systematic Investigation of Silylation Materials for Recovery Use of Low- k Material Plasma Damage. *071502*.

(28) Baik, K.-H. Gas Phase Silylation in the Diffusion Enhanced Silylated Resist Process for Application to Sub-0.5 Mm Optical Lithography. *J. Vac. Sci. Technol. B Microelectron. Nanom. Struct.* **1990**, *8* (6), 1481.

(29) Crowe, L. L.; Tolbert, L. M. Silica Passivation Efficiency Monitored by a Surface-Bound Fluorescent Dye. *Langmuir* **2008**, *24* (16), 8541–8546.

(30) Haukka, S.; Root, A. The Reaction of Hexamethyldisilazane and Subsequent Oxidation of Trimethylsilyl Groups on Silica Studied by Solid-State NMR and FTIR. *J. Physial Chem.* **1994**, *98* (6), 1695–1703.

(31) Sindorf, D. W.; Maciel, G. E. Cross-Polarization/Magic-Angle-Spinning Silicon-29 Nuclear Magnetic Resonance Study of Silica Gel Using Trimethylsilane Bonding as a Probe of Surface Geometry and Reactivity. *J. Phys. Chem.* **1982**, *86* (26), 5208–5219.

(32) Sneh, O.; George, S. M. Thermal Stability of Hydroxyl Groups on a Well-Defined Silica Surface. *J. Phys. Chem.* **1995**, *99* (13), 4639–4647.

(33) Boehm, H.-P. The Chemistry of Silica. Solubility, Polymerization, Colloid and Surface Properties, and Biochemistry. VonR. K. Iler. John Wiley and Sons, Chichester 1979. XXIV, 886 S., Geb. £ 39.50. *Angew. Chemie* **1980**, *92* (4), 328–328.

(34) Chang, H.-C.; Wang, L.-C. *A Simple Proof of Thue's Theorem on Circle Packing*.

(35) Iodinated Radiopharmaceuticals. In *RADIOIONIDATION REACTIONS FOR RADIO PHARMACEUTICALS*; Springer Netherlands: Dordrecht, 2006; pp 17–28.

(36) Nyns, L.; Delabie, a.; Caymax, M.; Heyns, M. M.; Van Elshocht, S.; Vinckier, C.; De Gendt, S. HfO[Sub 2] Atomic Layer Deposition Using HfCl[Sub 4]∕H[Sub 2]O: The First Reaction Cycle. *J. Electrochem. Soc.* **2008**, *155* (12), G269.

(37) Zhuravlev, L. T. *The Surface Chemistry of Amorphous Silica. Zhuravlev Model*; 2000; Vol. 173.

(38) Petrovykh, D. Y.; Sullivan, J. M.; Whitman, L. J. Quantification of Discrete Oxide and Sulfur Layers on Sulfur-Passivated InAs by XPS. *Surf. Interface Anal.* **2005**, *37* (11), 989–997.

(39) Hair, M. L.; Hertl, W. *Reactions of Chlorosilanes with Silica Surfaces*.

(40) Parsons, G. N. Functional Model for Analysis of ALD Nucleation and Quantification of Area-Selective Deposition. *J. Vac. Sci. Technol. A* **2019**, *37* (2), 020911.

(41) Popovici, M.; Groven, B.; Marcoen, K.; Phung, Q. M.; Dutta, S.; Swerts, J.; Meersschaut, J.; Van Den Berg, J. A.; Franquet, A.; Moussa, A.; et al. Atomic Layer Deposition of Ruthenium Thin Films from (Ethylbenzyl) (1-Ethyl-1,4-Cyclohexadienyl) Ru: Process Characteristics, Surface Chemistry, and Film Properties. *Chem. Mater.* **2017**, *29* (11), 4654–4666.

(42) Carlsson, J.-O. Selective Vapor-Phase Deposition on Patterned Substrates. *Crit. Rev. Solid State Mater. Sci.* **1990**, *16* (3), 161–212.

(43) Kern, W. The Evolution of Silicon Wafer Cleaning Technology. *J. Electrochem. Soc.* **1990**, *137* (6), 1887.

(44) Mackus, A. J. M.; Merkx, M. J. M.; Kessels, W. M. M. From the Bottom-Up: Toward Area-Selective Atomic Layer Deposition with High Selectivity †. *Chem. Mater.* **2018**, *31*, 2–12.